

mRNA vaccine quality analysis using RNA sequencing.

Helen M. Gunter^{1,2*}, Senel Idrisoglu^{1,2*}, Swati Singh^{1,2}, Dae Jong Han², Emily Ariens², Jonathan Peters², Ted Wong³, Seth W. Cheetham^{1,2}, Jun Xu⁴, Subash Kumar Rai⁴, Robert Feldman⁵, Andy Herbert⁵, Esteban Marcellin¹, Romain Tropee², Trent Munro^{1,2} and Tim R. Mercer^{1,2}

¹ Australian Institute for Bioengineering and Nanotechnology, University of Queensland, Australia

² BASE facility, University of Queensland, Australia

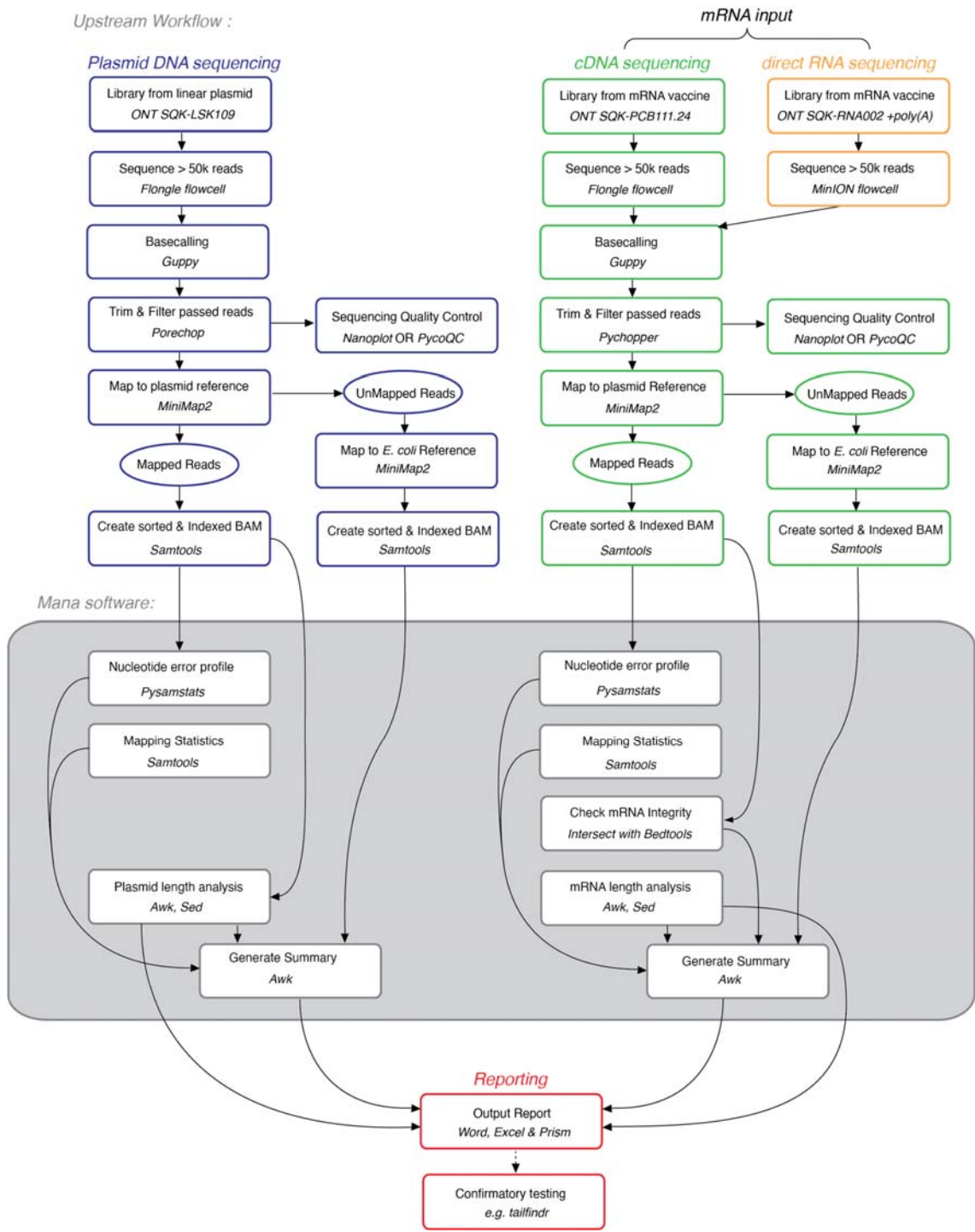
³ Garvan Institute of Medical Research

⁴ Genome Innovation Hub, University of Queensland, Australia

⁵ COVID19 Vaccine Corporation Limited (CVC), Auckland, New Zealand

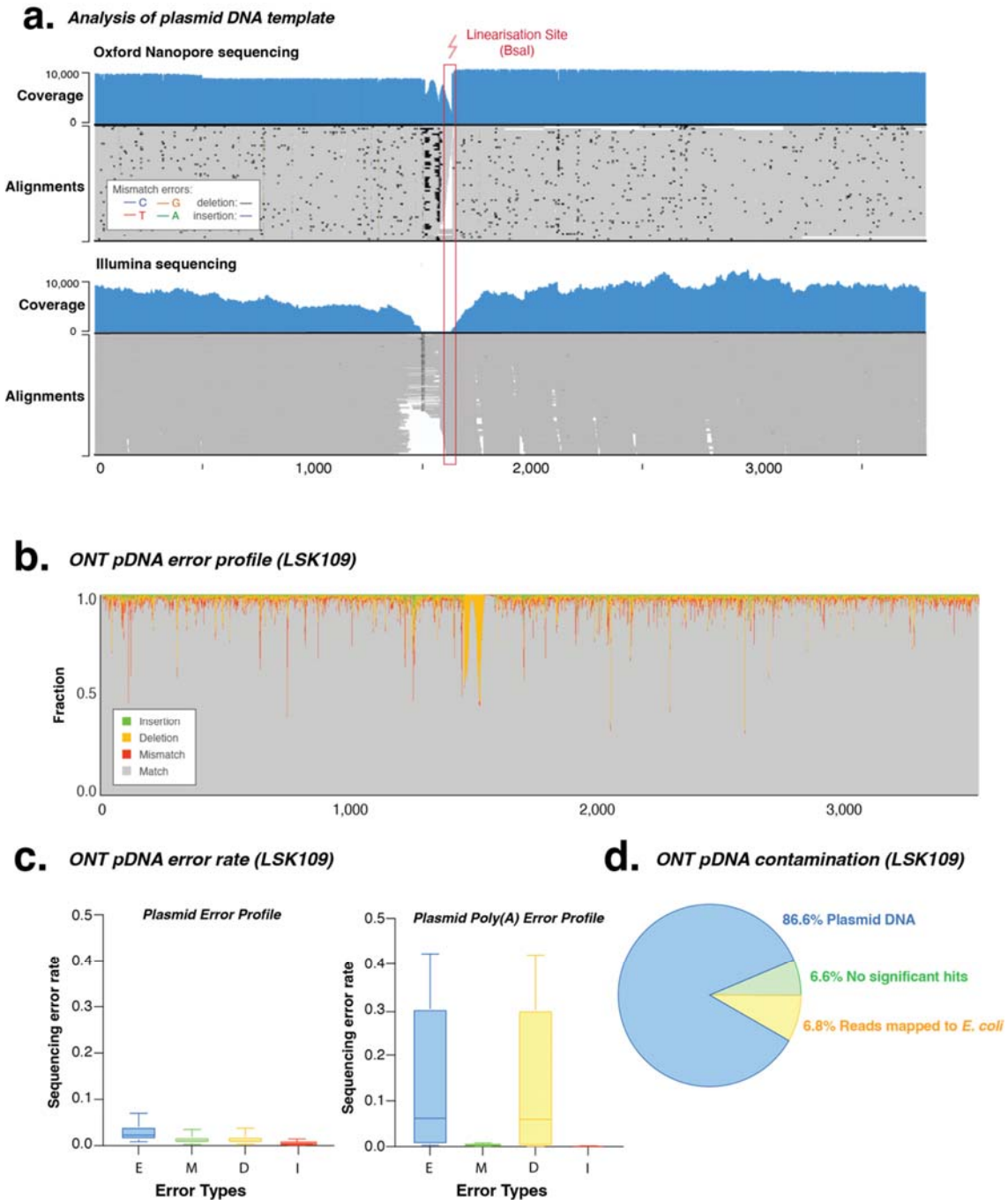
* These authors contributed equally.

Supplementary Figures 1-12



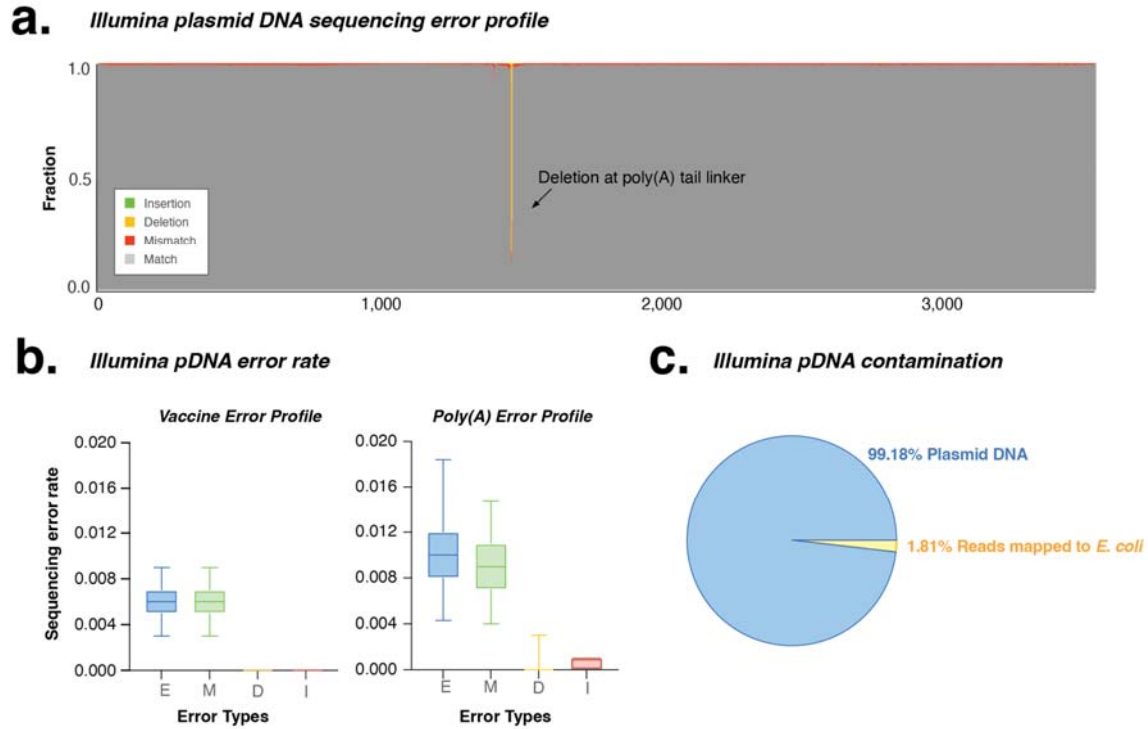
14

15 **Supplementary Figure 1. VAX-seq pipeline, including laboratory, manual bioinformatic and *Mana* software**
16 **analysis.** Briefly, ONT libraries are prepared from linearised plasmid, cDNA and directly from mRNA, and are
17 sequenced on either a Flongle or MinION flowcell. Reads are base-called, trimmed and aligned to the plasmid
18 reference genome. Unmapped reads are aligned to the *E. coli* genome, to quantify any contamination from the
19 plasmid preparation. Next, the *Mana* software utilises a range of software tools to compile a comprehensive
20 report on the proportion of on target, truncated and extended mRNA transcripts. This information can be used
21 to plan further analyses (such as *tailfinder*), optimise *in vitro* transcription workflows, and recommend whether
22 an mRNA is suitable for use. Source data are provided as a Source Data file.



23

24 **Supplementary Figure 2. Validation of Plasmid DNA quality using Oxford Nanopore Sequencing.** (a) Genome-
 25 browser (IGV) view of long-read (ONT) and short-read (Illumina) alignments across sequenced plasmid DNA
 26 template, with linearisation site indicated (red box). Coverage indicates the number of reads at each nucleotide
 27 position whilst the lower alignments grey bars indicate unique, individual alignments, with colouring indicating
 28 their similarity to the reference genome. (b) Sequencing profile showing error type and frequency across the
 29 plasmid DNA template. (c) Box and whisker plots summarise the per nucleotide error rates within the mRNA
 30 vaccine and poly(A) tail sequence (E total errors, M mismatch, D deletion and I insertion). Box extends from 25th
 31 to 75th percentile, whiskers extend 10 – 90th percentile, centre plotted at median. Sequencing data derived from
 32 n=1 replicates. (d) Pie-chart shows the proportion of DNA contamination detected in linearised plasmid DNA
 33 preparations as measured using Oxford Nanopore sequencing. Source data are provided as a Source Data file.



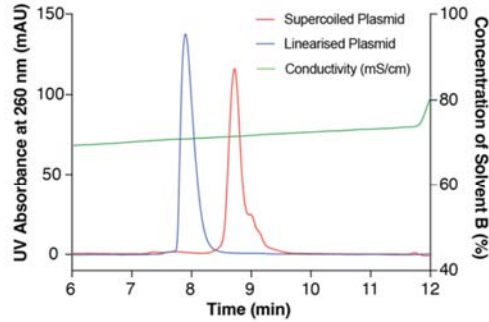
34

35 **Supplementary Figure 3. Validation of plasmid DNA quality using short-read (Illumina) sequencing.** (a)
 36 Sequencing profile shows error type and frequency across plasmid DNA template sequence. (b) Box and whisker
 37 plots show short-read sequencing per nucleotide error rates within the mRNA vaccine and poly(A) tail sequence.
 38 Box extends from 25th to 75th percentile, whiskers extend 10 – 90th percentile, centre plotted at median.
 39 Sequencing data derived from n=1 replicates. (c) Pie-chart illustrates the proportion of DNA contamination
 40 detected in plasmid sequencing libraries using Illumina sequencing. Source data are provided as a Source Data
 41 file.

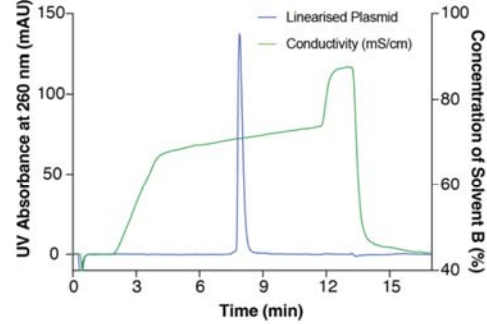
42

43

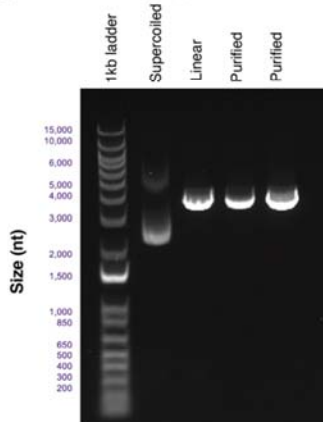
a. Plasmid linearisation (HPLC)



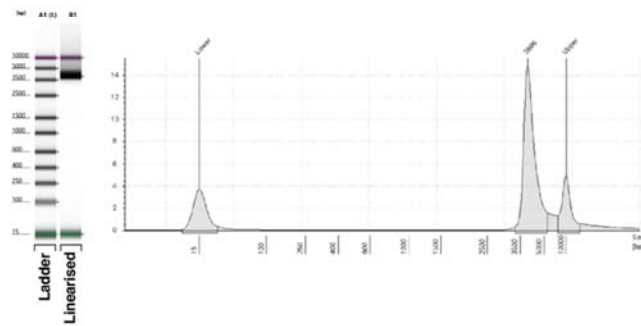
b. Plasmid linearisation (HPLC)



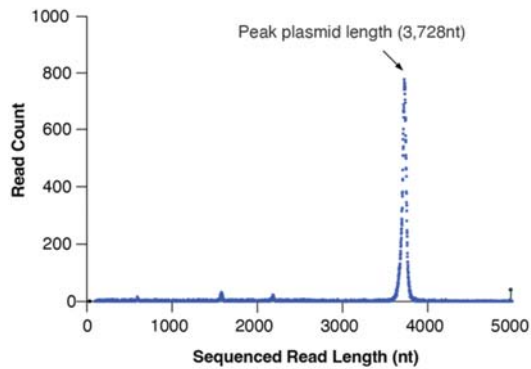
c. Plasmid size (gel electrophoresis)



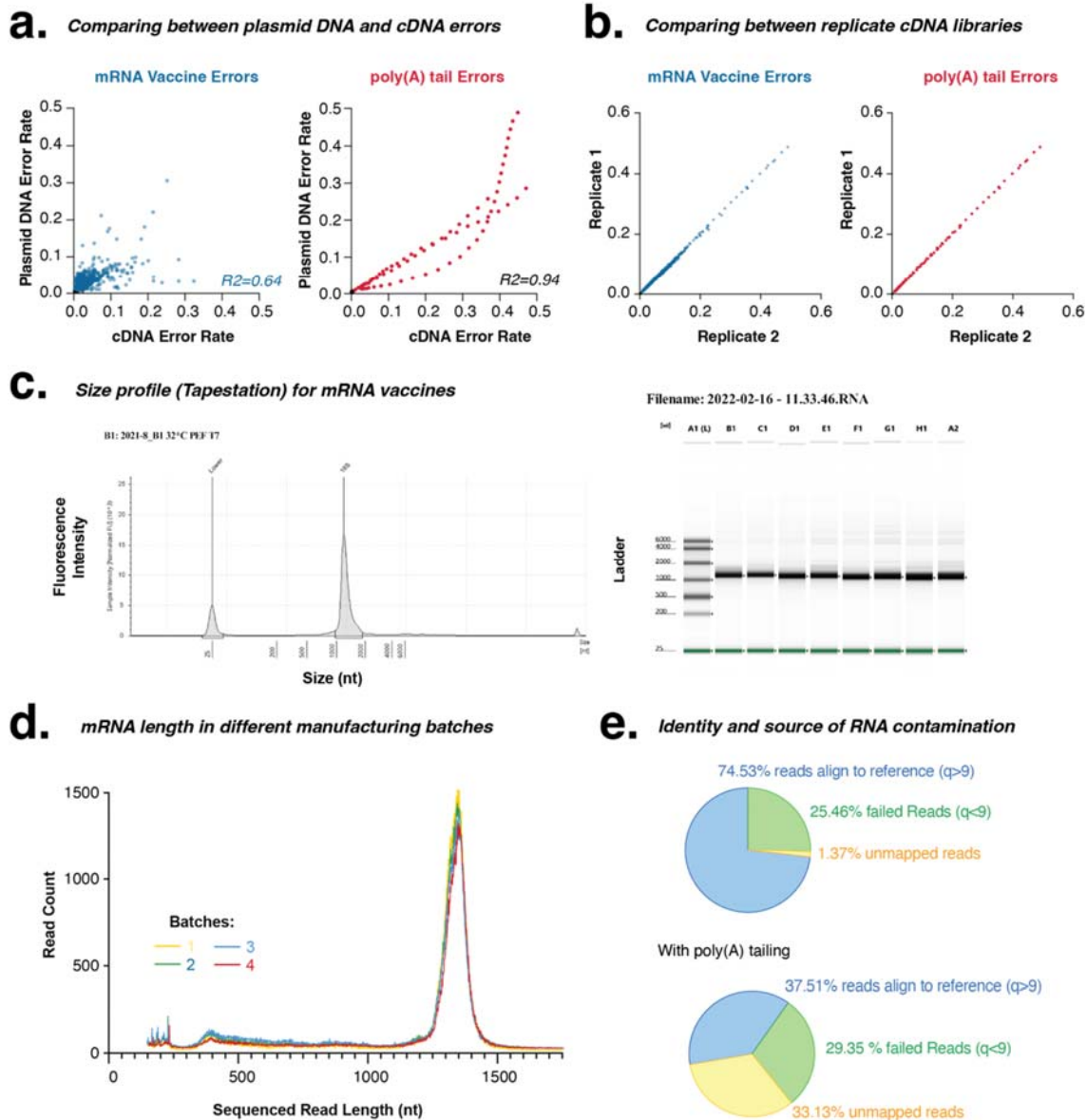
d. Linearised plasmid size (Tapestation)



e. Plasmid size (ONT sequencing)



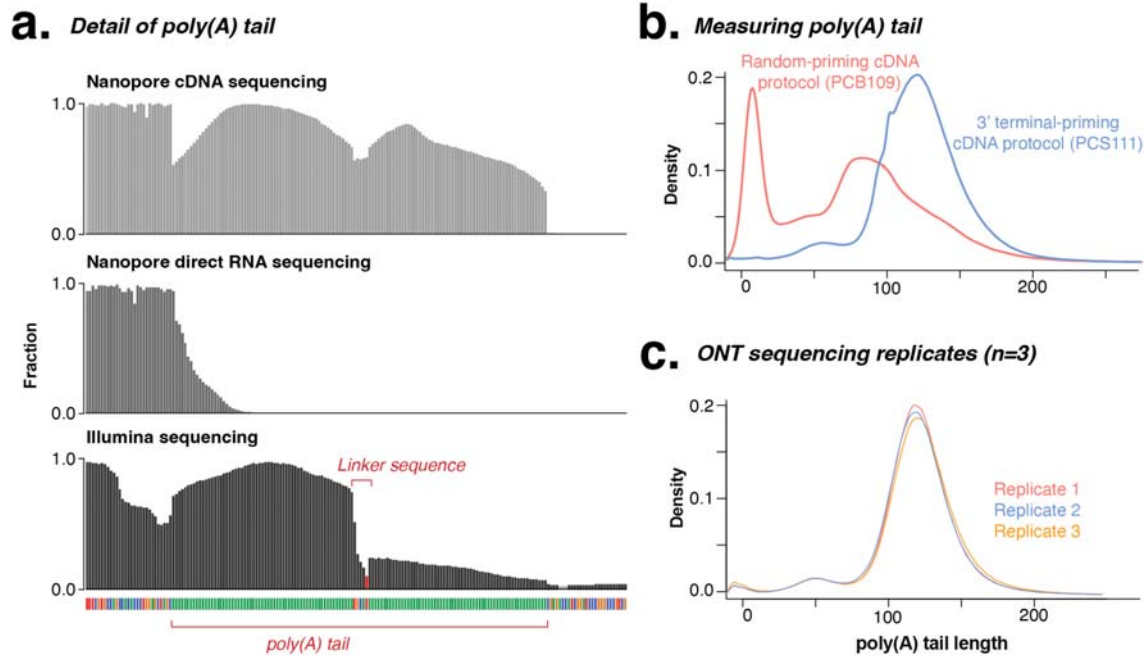
Supplementary Figure 4. Validation of plasmid length and linearisation. (a) High-performance liquid chromatography (HPLC) elution profile for coiled and linearized plasmids. (b) Linearisation efficiency as measured by HPLC analysis. (c) Agarose gel electrophoresis showing coiled, linearized and purified plasmid DNA preparations (n=1 supercoiled, n=1 linear, n=2 purified). (d) Analysis of linearized plasmid preparation using Agilent TapeStation shows size profile of plasmid preparations (n=1). (e) Size profile of linearised plasmid length as measured using long-read Oxford Nanopore sequencing. Source data are provided as a Source Data file.



53

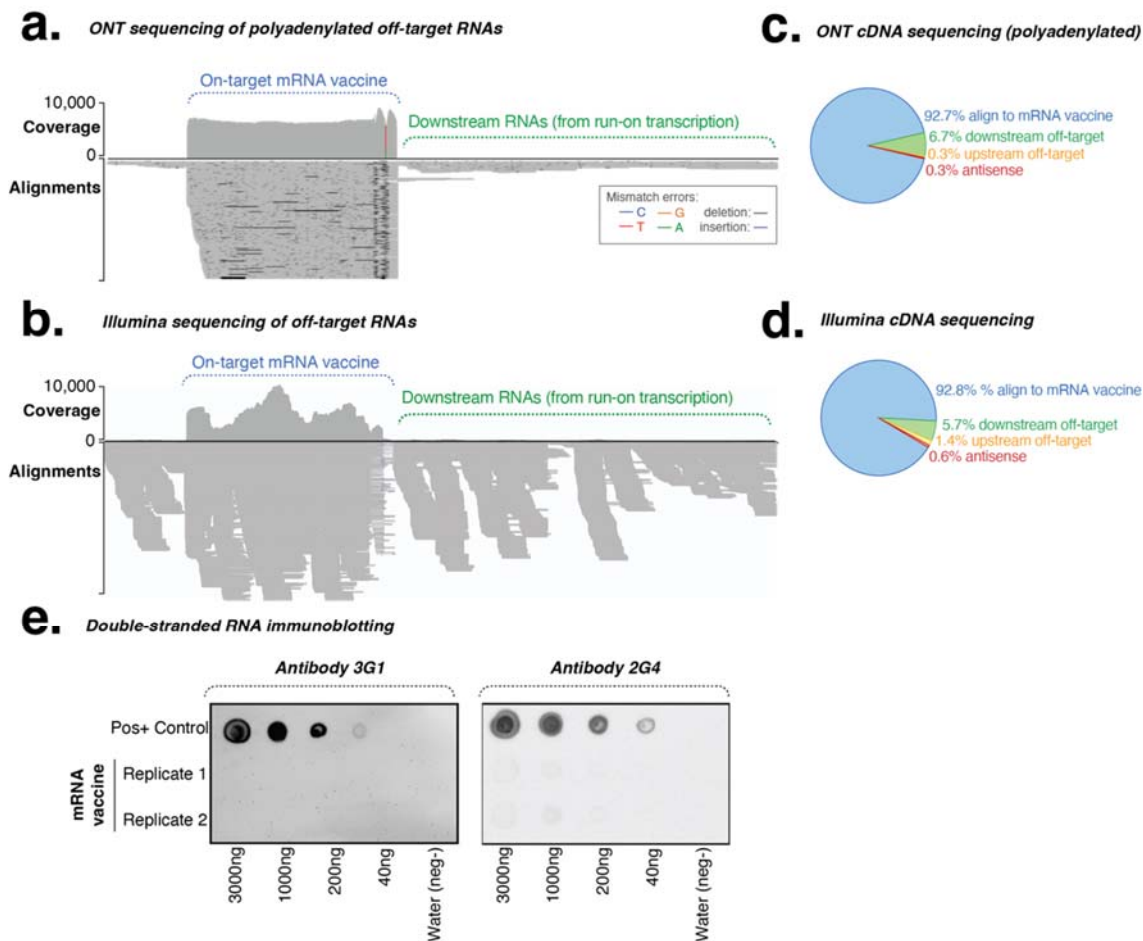
54 **Supplementary Figure 5. Sequencing error rate.** (a) Scatter-plot shows per-nucleotide comparison of error rate
55 between cDNA and plasmid DNA sequencing within the mRNA vaccine sequence (blue) and poly(A) tail (red). (b)
56 Per-nucleotide pairwise comparison of sequencing error-rates between technical sequencing replicates in mRNA
57 vaccine sequence (blue) and poly(A) tail (red). (c) Capillary electrophoresis size profile of reference eGFP mRNA
58 vaccines (as measured with Agilent TapeStation) shows size profile (left) and capillary electrophoresis bands for
59 replicate eGFP mRNAs transcribed from single plasmid preparation (right), (n=4). (d) Size plot generated from
60 using long-read sequences shows the reproducibility for measuring mRNA length across multiple different
61 manufacturing batches. (e) Pie chart shows the proportion of different contaminants as measured using long-
62 read sequencing in mRNA vaccine samples (top) and samples that have undergone additional polyadenylation
63 (bottom). Source data are provided as a Source Data file.

64



65

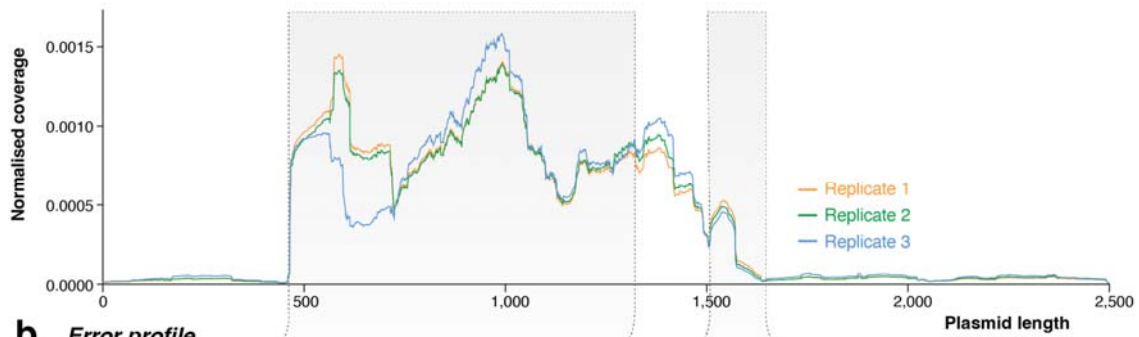
66 **Supplementary Figure 6. Detail of poly(A) tail.** (a) Detail shows alignment coverage at poly(A) tail for nanopore
67 cDNA (top), direct RNA (middle) and Illumina (lower) sequencing. (b) Density plot shows the measurement of
68 poly(A) tail length using *tailfindr* for the 3' terminal-priming cDNA (blue) and random-priming cDNA (red)
69 sequencing protocols. (c) Density plot shows the reproducibility of measuring poly(A) tail length across technical
70 replicates (n=3). Source data are provided as a Source Data file.



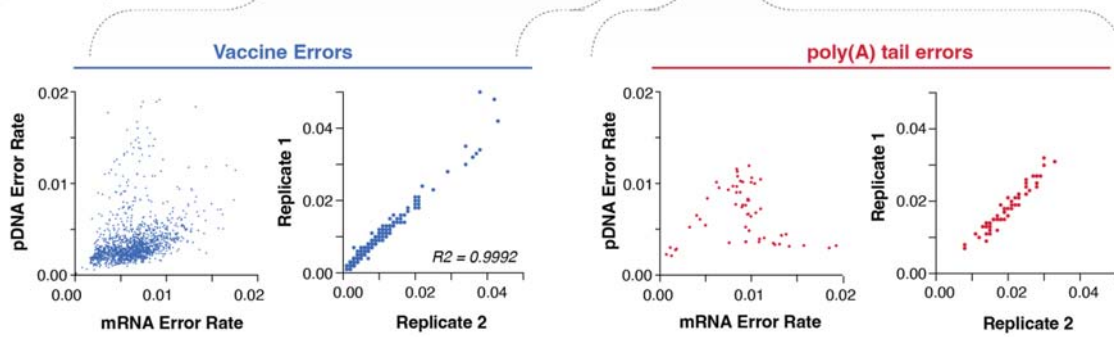
71

72 **Supplementary Figure 7. Analysis of off-target RNA contamination.** Genome browser view shows off-target
73 RNA transcripts generated from cryptic transcription initiation or readthrough transcription for **(a)** long-read
74 (following additional polyadenylation) or **(b)** short-read sequencing. Coverage indicates the number of reads at
75 each nucleotide position whilst the lower alignments grey bars indicate unique, individual alignments, with
76 colouring indicating their similarity to the reference genome. Pie-chart shows the composition of RNA
77 contamination in mRNA samples as measured within **(c)** long- and **(d)** short-read sequencing libraries. **(e)** dsRNA
78 immunoblotting using two different dsRNA-specific antibodies to detect the presence of double-stranded RNAs
79 in mRNA vaccine samples. The dsRNA positive control was generated from previous manufacture⁴⁴. Source data
80 are provided as a Source Data file.

a. Short-read alignment coverage

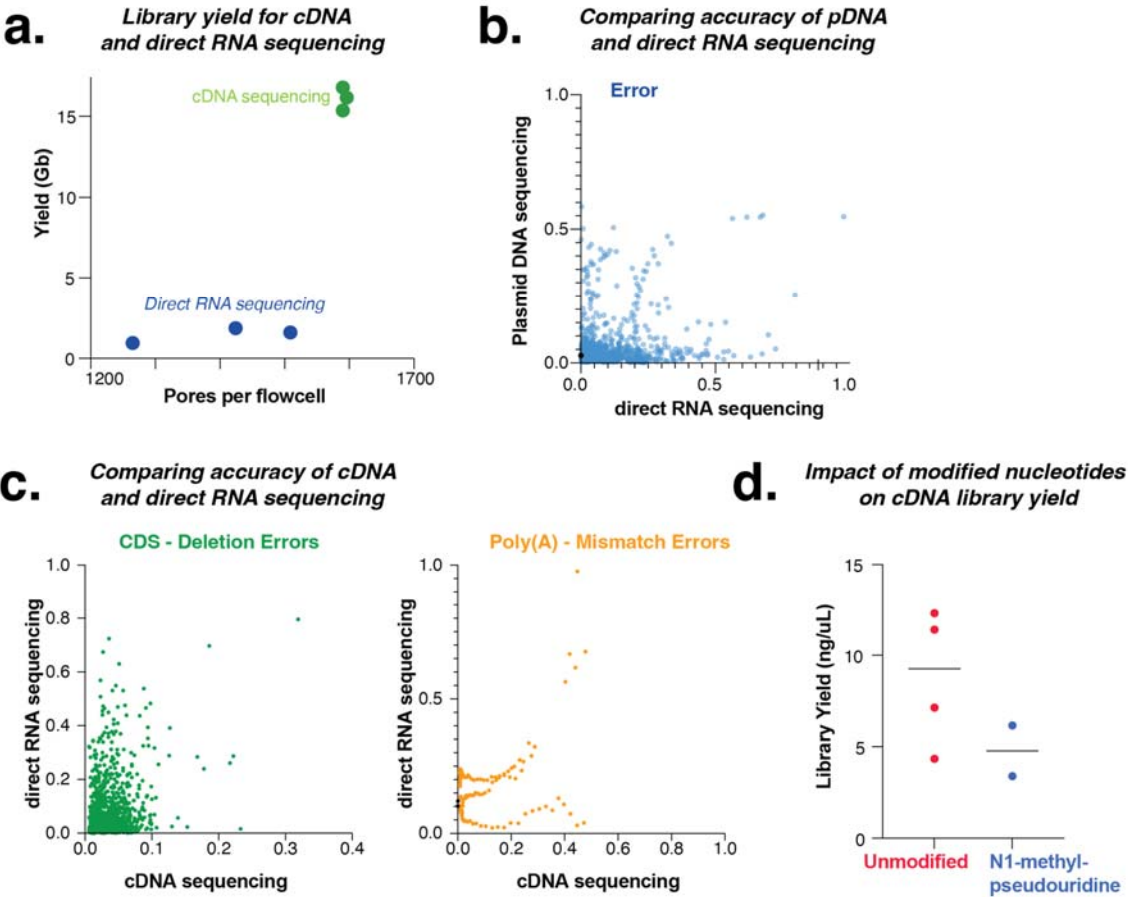


b. Error profile



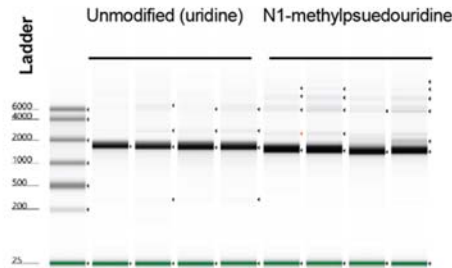
81

82 **Supplementary Figure 8. Short-read Illumina sequencing of mRNA vaccine.** (a) Histogram plot shows short-read
 83 alignment for an mRNA vaccine across replicate batches (n=3) showing reproducibility of alignment
 84 coverage. (b) Scatter plots compare per-nucleotide error rate in cDNA sequencing relative to plasmid DNA
 85 sequencing in an mRNA vaccine sequence (blue) and poly(A) tails (red), and per-nucleotide error frequency
 86 between replicate mRNA batches. Source data are provided as a Source Data file.

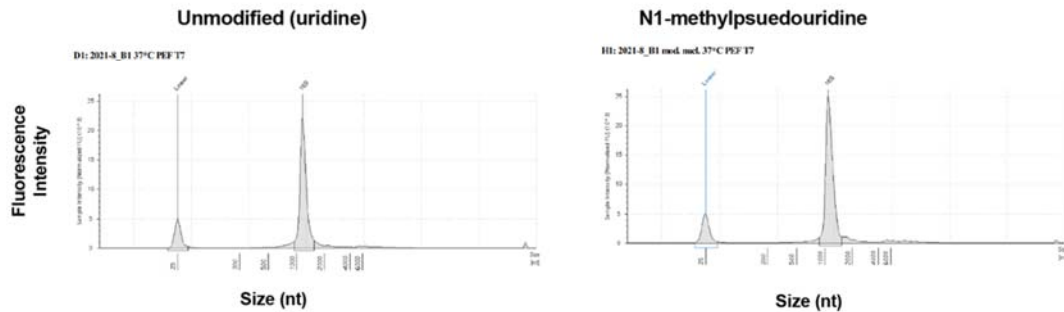


Supplementary Figure 9. Direct RNA sequencing of mRNA vaccines. (a) Scatter plot displaying the yield of libraries obtained from cDNA and direct RNA sequencing. (b) Scatter plot compares per-nucleotide error-rates between plasmid DNA and direct RNA sequencing in an mRNA vaccine. (c) Scatter plot compares per-nucleotide error rates between cDNA and direct RNA sequencing in the mRNA vaccine (green) and poly(A) tail (orange). (d) Comparison of cDNA library-yield between unmodified (red) and modified (blue; N1-methylpseudouridine) mRNA vaccines. (n=4 for unmodified libraries, and n=2 for modified libraries). Source data are provided as a Source Data file.

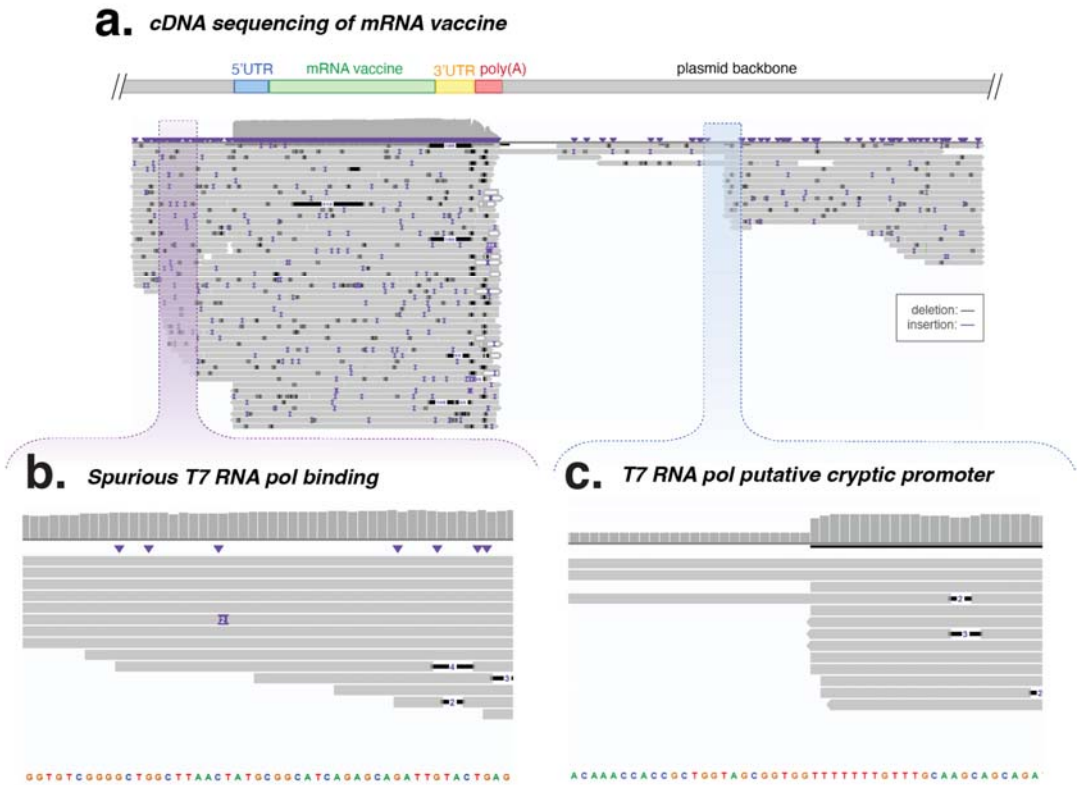
a. Size profile (Tapestation) for modified mRNA vaccines



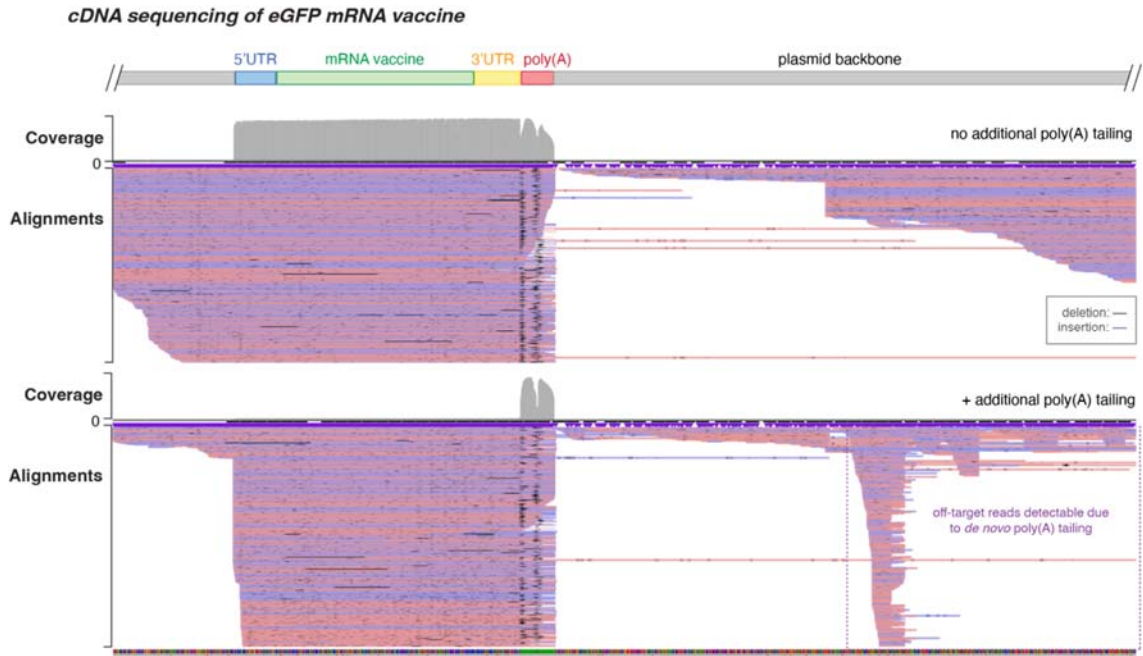
b. Example profile (Tapestation) for modified mRNA vaccines



Supplementary Figure 10. Electrophoresis (Agilent TapeStation) size analysis of modified (N1-methylpseudouridine) mRNA vaccine. (a) Gel electrophoresis shows shorter migration of modified mRNA vaccines compared to unmodified mRNA vaccines in comparison to TapeStation RNA ladder (n=4). **(b)** Example size profiles for individual unmodified (left) and modified (right) mRNA vaccines. Source data are provided as a Source Data file.



Supplementary Figure 11. Potential off-target binding of T7 RNA polymerase in an mRNA vaccine. (a) Genome browser view shows off-target transcripts identified by long-read sequencing of *in vitro* transcribed mRNA vaccine. (b) Off-target transcripts likely generated through spurious T7 RNA polymerase binding, 5' to the T7 promoter included in our construct. (c) Additionally, a potential cryptic T7 promoter was identified, where transcription appears to have been initiated at the same position for eight reads, potentially due to the presence of a polypyrimidine tract. T7 promoter binding affinity at this position could be tested by DNA foot-printing analyses. Source data are provided as a Source Data file.



Supplementary Figure 12. *De novo* poly(A) tailing of eGFP mRNA permits detection of additional off-target transcripts. Genome browser view comparing ONT cDNA sequencing libraries that include additional poly(A) tailing (bottom panel) to libraries that lack additional poly(A) tailing (top panel). Additional off-target transcripts are observed in libraries with *de novo* poly(A) tailing in comparison to those without *de novo* poly(A) tailing, as cDNA sequencing libraries involve a poly(A) selection step. Source data are provided as a Source Data file.

Source Data files

Figure S4c

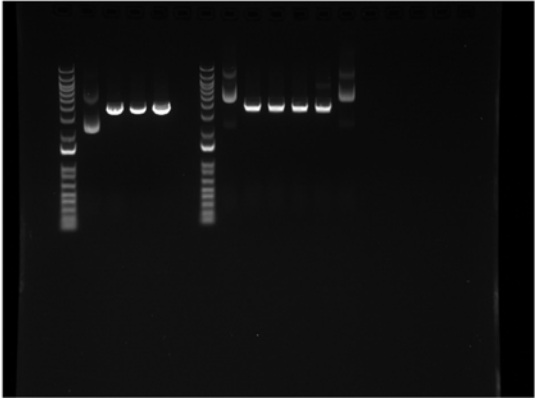


Figure S4d

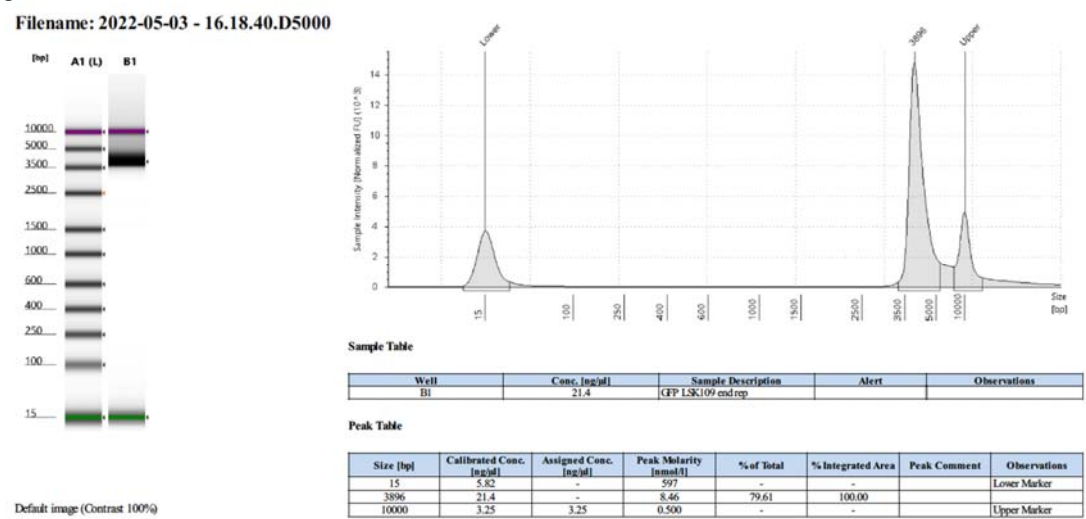
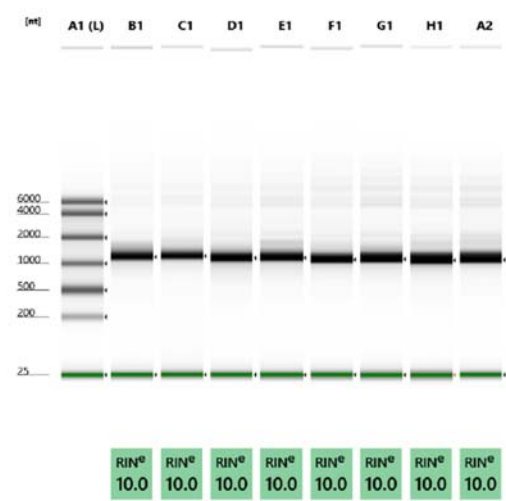


Figure S5c, S10a
Filename: 2022-02-16 - 11.33.46.RNA



Default image (Contrast 100%)
Figure S7e: 3G1 antibody

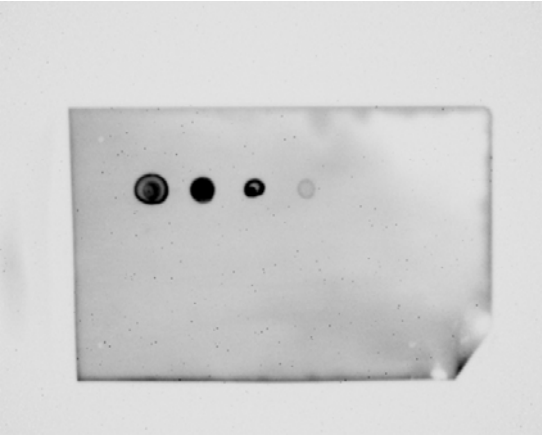


Figure S7e: 2G4 antibody

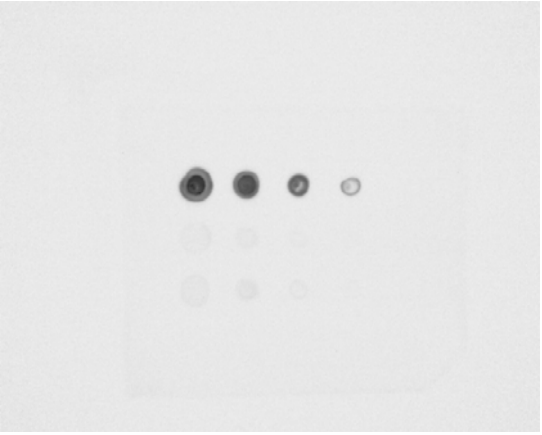
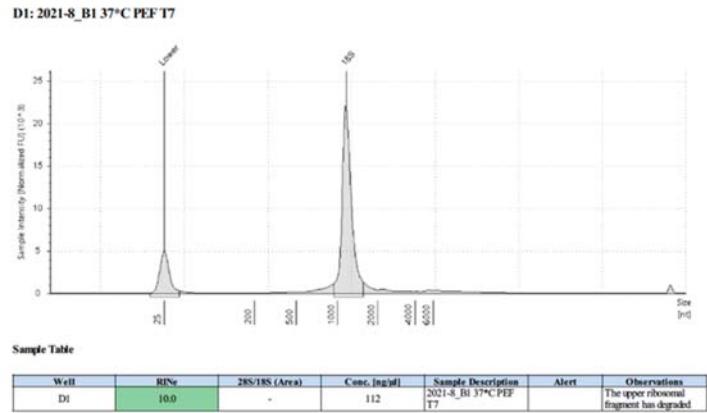
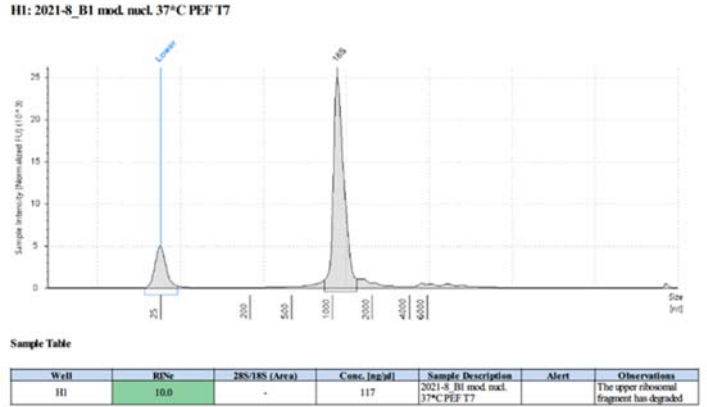


Figure S10b



Peak Table

Size [nt]	Calibrated Conc. [ng/μl]	Assigned Conc. [ng/μl]	Peak Molarity [nmol/l]	% Integrated Area	Peak Comment	Observations
25	36.0	36.0	4240	-		Lower Marker
1160	85.4	-	217	100.00		18S



Peak Table

Size [nt]	Calibrated Conc. [ng/μl]	Assigned Conc. [ng/μl]	Peak Molarity [nmol/l]	% Integrated Area	Peak Comment	Observations
25	36.0	36.0	4240	-		Lower Marker
1090	94.1	-	254	100.00		18S